Guided modes in asymmetric metal-cladding left-handed material waveguides

Ying He (何 英)*, Xia Zhang (张 霞), Yanfang Yang (杨艳芳), and Chunfang Li (李春芳)

Department of Physics, Shanghai University, Shanghai 200444, China

**Corresponding author: heying@staff.shu.edu.cn*

Received October 9, 2010; accepted December 14, 2010; posted online April 18, 2011

We investigate guided modes in the asymmetric waveguide structure with a left-handed material (LHM) layer surrounded by air and metal. A graphical method is proposed to determine the guided modes. New properties of the oscillating and surface guided modes, such as absence of the fundamental mode, coexistence of the oscillating and surface guided modes, fast attenuation of the surface guided modes, and mode degeneracy, are analyzed in detail. We also investigate dispersive characteristics of the metal-LHM-air optical waveguide. The propagation constant increases with decreasing slab thickness for the first-order oscillating mode, which is different from that in traditional metal-cladding waveguides.

OCIS codes: 230.7390, 260.2030, 260.3910.

doi: 10.3788/COL201109.052301.

Negative refractive index materials exhibit both negative dielectric permittivity and negative magnetic permeability, and thus possess a negative refractive index as Veselago first predicted theoretically in 1968[1]. Since electric and magnetic fields form a left set of vectors with the wave vector, the novel materials are also called left-handed materials (LHMs). Metamaterials are a special class of negative refractive index materials with artificial electromagnetic properties defined by their subwavelength structure. They are characterized by an effective negative refraction index that gives rise to extraordinary properties such as backwards phase propagation and negative refraction. The nonlinear effect in LHMs has been investigated recently[2]. These unusual properties open up many possibilities for a wide range of applications, including invisibility cloaking[3], sub-diffraction imaging[4,5], and microstrip patch antenna[6]. LHMs have been realized through layering of resonant structures and by using waveguides[7,8].

During the last decade, plasma utilizing surface plasmon polaritons (SPPs) supported at the metal-dielectric interface has been attracting much renewed attention worldwide. Metal-cladding waveguides have many applications due to their capacity to sustain SPP modes. The confined SPPs in metal-insulator-metal waveguides can act as an integrated electrical source[9]. Plasmonic filters based on the metal-insulator-metal waveguides have been studied widely. In the case of metal-dielectric-metal waveguides, they open up many possibilities for a wide range of applications, including power splitters[10], novel nanometeric plasmonic refraction index sensor[11], and waveguide couplers[12].

Electromagnetic energy guidance in various structures, including LHMs, is fundamental in photonic devices. Guided modes in waveguides provide vital information for future applications. Metal-LHM-dielectric waveguide is a useful structure for electromagnetic energy transmission. SPPs can be supported at the metal-LHM interface and the LHM-dielectric interface[13]. While the symmetric and asymmetric three-layer left-handed waveguides have been investigated[14−19] and potential applications have been put forward[20], the metal-LHM-dielectric structure seems less studied. In this letter, we consider the guided modes in an asymmetric three-layer slab waveguide with a LHM layer surrounded by metal and air. The graphical method is used to determine the guided modes. Theoretical dispersive characteristics of the metal-LHM-dielectric waveguide are presented.

An asymmetric metal-cladding waveguide structure is shown in Fig. 1 with a LHM layer of width d surrounded by semi-infinite air and metal. The LHM layer has negative permittivity ε_1 and negative permeability μ_1. The metal has negative permittivity ε_3 and positive permeability μ_3. For the transverse electric (TE) wave, the electric field E is polarized along the y axis. Time dependence of the monochromatic field is expressed as $\exp(-\mathrm{i}wt)$. The form of the mode propagating in the z direction is $E(x)\exp[-\mathrm{i}(wt-\beta z)]$, where β is the propagation constant.

Electric field components in the three layers can be written as

$$E_1(x) = B\mathrm{e}^{-\mathrm{i}\kappa_1 x} + C\mathrm{e}^{\mathrm{i}\kappa_1 x} (0 < x < d), \tag{1}$$

$$E_2(x) = D\mathrm{e}^{-P_2(x-d)} (x > d), \tag{2}$$

$$E_3(x) = A\mathrm{e}^{P_3 x} (x < 0), \tag{3}$$

where P_2 and P_3 are evanescent coefficients corresponding to the two claddings, which can be written as

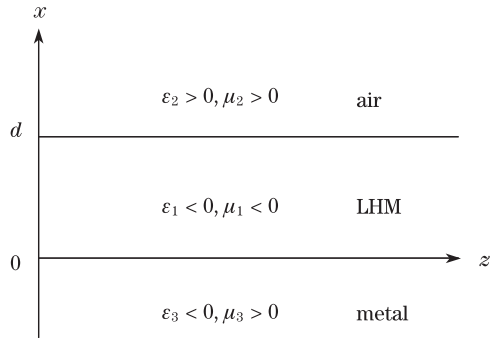

Fig. 1. Geometry and notations for an asymmetric metal-cladding waveguide with LHM layer.

 © 2011 Chinese Optics Letters

$P_2 = \sqrt{\beta^2 - k_0^2\varepsilon_2\mu_2}$ and $P_3 = \sqrt{\beta^2 - k_0^2\varepsilon_3\mu_3}$, respectively; κ_1 is the transverse wave number in the waveguide layer region, which can be expressed as $\kappa_1 = \sqrt{k_0^2\varepsilon_1\mu_1 - \beta^2}$; k_0 represents the vacuum wave number, and β is the propagation constant.

We match the corresponding boundary conditions at x=0 and x=d from Eqs. (1)–(3) and obtain the dispersion equation

$$\tan(\kappa_1 d) = \frac{\frac{\mu_1}{\mu_3}\frac{P_3}{\kappa_1} + \frac{\mu_1}{\mu_2}\frac{P_2}{\kappa_1}}{1 - \frac{\mu_1}{\mu_3}\frac{P_3}{\kappa_1}\frac{\mu_1}{\mu_2}\frac{P_2}{\kappa_1}}. \tag{4}$$

When κ_1 is real, allowable eigenmodes from Eq. (4) are oscillating guided modes. To describe the right-hand side (RHS) of Eq. (4) as a function of $\kappa_1 d$ and facilitate the discussion about the guided modes, we set

$$P_2 = \sqrt{k_0^2(\varepsilon_1\mu_1 - \varepsilon_2\mu_2) - \kappa_1^2},$$
$$P_3 = \sqrt{k_0^2(\varepsilon_1\mu_1 - \varepsilon_3\mu_3) - \kappa_1^2}. \tag{5}$$

With these notations in Eq. (5), the RHS of Eq. (4) becomes

$$F(\kappa_1 d) = \kappa_1 d \frac{\frac{\mu_2}{\mu_1}\sqrt{a^2 - (\kappa_1 d)^2} + \frac{\mu_3}{\mu_1}\sqrt{b^2 - (\kappa_1 d)^2}}{(\kappa_1 d)^2\frac{\mu_2\mu_3}{\mu_1^2} - \sqrt{a^2 - (\kappa_1 d)^2}\sqrt{b^2 - (\kappa_1 d)^2}}, \tag{6}$$

where $a = k_0 d\sqrt{\varepsilon_1\mu_1 - \varepsilon_2\mu_2}$, $b = k_0 d\sqrt{\varepsilon_1\mu_1 - \varepsilon_3\mu_3}$.

Wave number κ_1 becomes purely imaginary when propagation constant β exceeds a critical value, i.e., $k_1 = \mathrm{i}\alpha_1$. In this case, determining the eigenmodes becomes

$$\tanh(\alpha_1 d) = -\frac{\frac{\mu_1}{\mu_3}\frac{P_3}{\alpha_1} + \frac{\mu_1}{\mu_2}\frac{P_2}{\alpha_1}}{1 + \frac{\mu_1}{\mu_3}\frac{P_3}{\alpha_1}\frac{\mu_1}{\mu_2}\frac{P_2}{\alpha_1}}. \tag{7}$$

Similarly, the RHS of Eq. (7) is defined as

$$G(\alpha_1 d) = -\alpha_1 d \frac{\frac{\mu_2}{\mu_1}\sqrt{a^2 + (\alpha_1 d)^2} + \frac{\mu_3}{\mu_1}\sqrt{b^2 + (\alpha_1 d)^2}}{(\alpha_1 d)^2\frac{\mu_2\mu_3}{\mu_1^2} + \sqrt{a^2 + (\alpha_1 d)^2}\sqrt{b^2 + (\alpha_1 d)^2}}. \tag{8}$$

Shelby *et al.* fabricated structured LHMs having a range of frequencies over which the refractive index was predicted to be negative[21]. These structures used split ring resonators to produce negative magnetic permeability over a particular frequency region, and wire elements to produce negative electric permittivity in an overlapping frequency region. Permittivity and permeability of the LHM layer can be obtained from the Drude model describing frequency dependencies of the structured LHM characteristics

$$\varepsilon_1(w) = 1 - w_\mathrm{p}^2/(w^2 + \mathrm{i}\gamma_1 w),$$
$$\mu_1(w) = 1 - F_1 w^2/(w^2 - w_0^2 + \mathrm{i}\Gamma_1 w), \tag{9}$$

where w_p and w_0 are the electronic and magnetic plasma frequencies, γ_1 and Γ_1 are the damping rates relating to the absorption of the material, F_1 is connected with the internal structure of the material, and w is the frequency of incident light. Parameters for the internal structures are $w_\mathrm{p} = 10.0$ GHz, $w_0 = 4.0$ GHz, $\gamma_1 = 0.03w_\mathrm{p}$, $\Gamma_1 = 0.03w_0$, and $F_1 = 0.56$. Permittivity and permeability of the LHM in the present waveguide structure can be achieved for different frequencies of incident light. Metal is one kind of single-negative material, and its parameters can also be obtained from the frequency dependencies of the negative electric permittivity.

Provided $k_0^2\varepsilon_1\mu_1 > \beta^2 > k_0^2\varepsilon_2\mu_2$, oscillating guided modes can exist in the LHM layer. Dispersion Eqs. (4) and (7) are transcendental and cannot be solved analytically. Therefore, we use a graphical method to determine the solution to $\kappa_1 d$ for the guided modes. We plot the $\tan(\kappa_1 d)$ and $F(\kappa_1 d)$ dependencies on $\kappa_1 d$ in Fig. 2. With the parameters we obtain from Eq. (9), the $\kappa_1 d$ corresponding to the intersections can be obtained from the graph directly. The intersections show the existence of the guided modes.

We can examine the shape of the corresponding field components. The transverse profiles, corresponding to the four guided modes in Fig. 2 (i.e., TE_2, TE_3, TE_4, and TE_5), are shown in Fig. 3. As these figures show, the electric field oscillates in the LHM layer and is evanescent outside the LHM region. The two peaks are clearly asymmetric in Fig. 3(a) due to the asymmetries of the

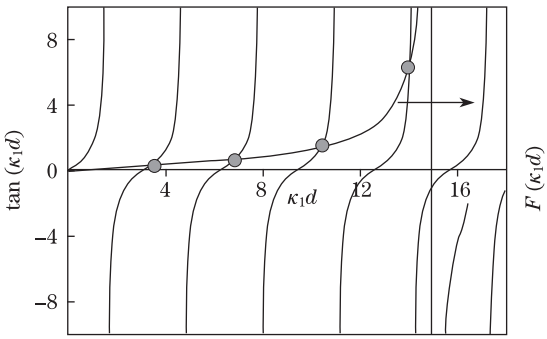

Fig. 2. Graphical determination of $\kappa_1 d$ for oscillating guided modes of an asymmetric metal-cladding waveguide with LHM layer. The parameters are $w = 4.6$ GHz, $a^2 = 1320$, $b^2 = 270$, $\varepsilon_1 = -3.7$, $\mu_1 = -1$; $\varepsilon_2 = 1$, $\mu_2 = 1$; $\varepsilon_3 = -9.5$, $\mu_3 = 1$.

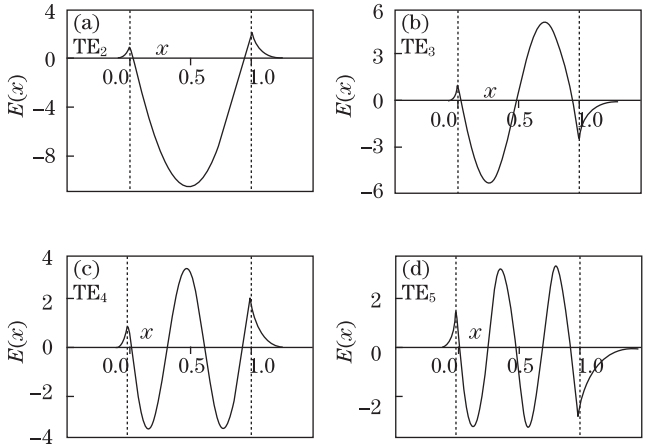

Fig. 3. Transverse profiles of the guided modes corresponding to the four intersections in Fig. 2. (a) TE_2: $\kappa_1 d = 3.45$; (b) TE_3: $\kappa_1 d = 6.91$; (c) TE_4: $\kappa_1 d = 10.40$; (d) TE_5: $\kappa_1 d = 13.98$.

structures. Electric field distributions of other guided modes are also asymmetric. For $w = 4.6$ GHz and $d = 1$, we cannot find the oscillating modes TE_1 and TE_0. TE_1 exists for some particular parameters. The fundamental mode TE_0 cannot be found for any parameters in the present LHM waveguide, which is different from the conventional metal cladding waveguide.

We plot the dependencies of $\tanh(\alpha_1 d)$ and $G(\alpha_1 d)$ on $\alpha_1 d$ for surface guided modes in Fig. 4. Intersections show the existence of surface modes. When the frequency of incident light 4.0 GHz $< w <$ 4.7 GHz, there is no intersection. For 5.1 GHz $< w <$ 6.0 GHz, there is only one intersection. For 4.7 GHz $< w \leq$ 5.1 GHz, there are two intersections.

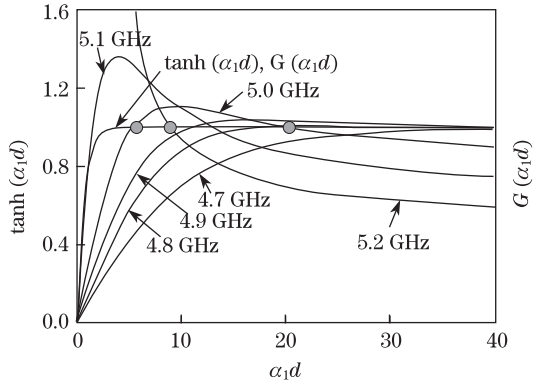

Fig. 4. Graphical determination of $\alpha_1 d$ for surface modes of asymmetric metal-cladding LHM waveguides with LHM layer for different frequencies. The parameters are (a) $w =$ 4.7 GHz, $a^2 = 1250$, $b^2 = 250$; (b) $w = 4.8$ GHz, $a^2 = 1144$, $b^2 = 164$; (c) $w = 4.9$ GHz, $a^2 = 1064$, $b^2 = 124$; (d) $w = 5.0$ GHz, $a^2 = 965$, $b^2 = 65$; (e) $w = 5.1$ GHz, $a^2 = 872$, $b^2 = 12$; (f) $w = 5.2$ GHz, $a^2 = 801$, $b^2 = -29$.

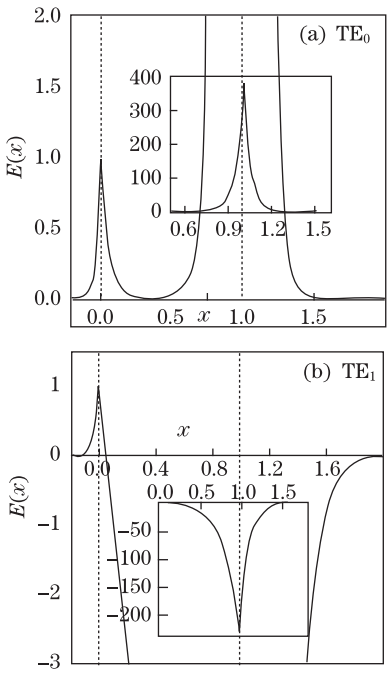

Fig. 5. Transverse profiles for surface guided modes corresponding to the two intersections in Fig. 4 for $w = 5.0$ GHz. (a) TE_0: $\alpha_1 d = 20.46$; (b) TE_1: $\alpha_1 d = 5.31$.

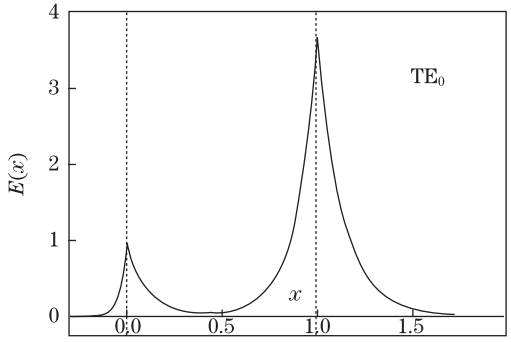

Fig. 6. Transverse profile for the surface guided mode corresponding to the intersection in Fig.4 for $w = 5.2$ GHz. TE_0: $\alpha_1 d = 8.90$.

For $w = 5.0$ GHz, there are two intersections. Electric field distributions corresponding to the two intersections of the surface modes are shown in Fig. 5. They are surface TE_0 and TE_1 modes. Field amplitudes evanesce exponentially in the slab region and outside the slab region for both surface modes. They evanesce quickly especially near the interface between the LHM and air, as seen in the insets of Fig. 5.

For $w = 5.2$ GHz, there is only one intersection (Fig. 4). The corresponding electric field distribution of the surface mode is plotted in Fig. 6.

To sum up, metal-LHM-air waveguide is a useful structure for the transmission of guided modes. Due to the SPPs supported at the metal-LHM interface and at the LHM-air interface, the metal-cladding left-handed waveguides support both oscillating and surface guided optical modes. The existence of various solutions on the surface guided modes depends on the frequency of incident light and the waveguide structure.

We discuss the dependence of the propagation constant β on the thickness d of the LHM layer in the asymmetric metal-cladding left-handed waveguides. We can take a comparison of the dispersive curves for the traditional metal-cladding and that for metal-cladding left-handed waveguides.

Dispersive curves of the traditional metal-cladding and metal-cladding left-handed waveguides are shown in Figs. 7 and 8, respectively. With the increase of propagation constants β, the slab thickness d decreases for the

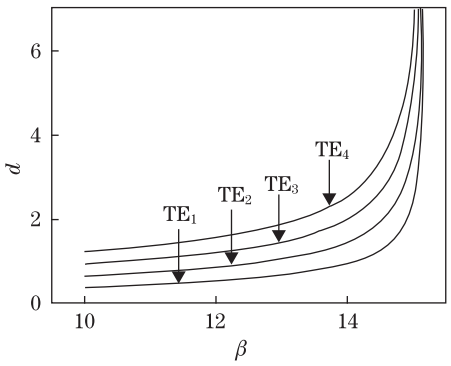

Fig. 7. Dispersive curves for TE guided modes of the metal-cladding waveguide with $w = 5.0$ GHz, $\varepsilon_1 = 2.31, \mu_1 = 1; \varepsilon_2 = 1, \mu_2 = 1; \varepsilon_3 = -8, \mu_3 = 1$.

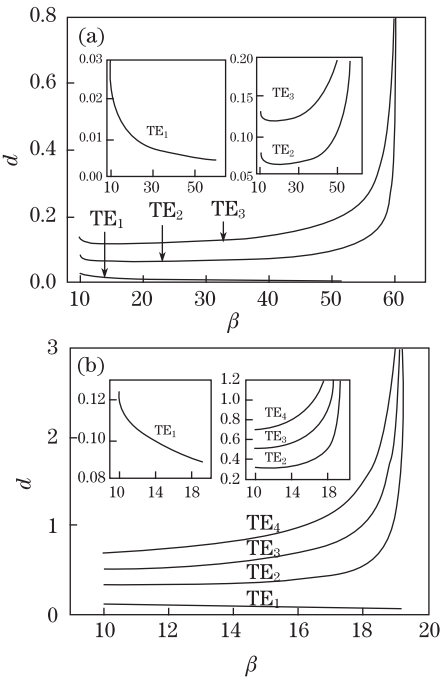

Fig. 8. Dispersive curves for TE guided modes of the metal-cladding left-handed waveguides when (a) ω = 4.1 GHz, ε_1 = –4.9, μ_1 = –7.5; ε_2 = 1, μ_2 = 1; ε_3 = –12, μ_3 = 1; (b) ω = 4.6 GHz, ε_1 = –3.7, μ_1 = –1; ε_2 = 1, μ_2 = 1; ε_3 = –9.5, μ_3 = 1.

oscillating mode TE_1, while the propagation constants increase with increasing slab thickness in the traditional metal-cladding waveguides. Furthermore, two different propagation constants β correspond to the same thickness d for the modes TE_2 and TE_3, which are shown in the inset in Fig. 8(a). Mode degeneracy appears in the metal-cladding left-handed waveguide, but does not always exist, as is shown in Fig. 8(b). Mode degeneracy depends on the waveguide structure, especially the permittivity and permeability of the LHM and metal.

In conclusion, asymmetric metal-cladding LHM waveguides are investigated in detail in the letter. The existence and new properties of the guided modes are analyzed with a graphical method. The waveguide supports both oscillating and surface guided modes. The existence of various solutions on the surface guided modes depends on the frequency of incident light and the waveguide structure. With the increase of propagation constants, the slab thickness decreases for the first-order oscillating mode. New properties in the air-LHM-metal waveguide may provide valuable information for its future applications in plasmonic filters and waveguide couplers.

This work was supported by the National Natural Science Foundation of China (Nos. 60806041 and 60877055) and the Innovation Funds for Graduates of Shanghai University (No. SHUCX102016).

References

1. V. G. Veselago, Sov. Phys. Usp. **10,** 509 (1968).
2. C. Zhou, Y. Gao, and Z. Liang, Acta Opt. Sin. (in Chinese) **30,** 2074 (2010).
3. T. Ergin, N. Stenger, P. Brenner, J. B. Pendry, and M. Wegener, Science **328,** 337 (2010).
4. J. B. Pendry, Phys. Rev. Lett. **85**, 3966 (2000).
5. S. Feng, C. Ren, D. Xu, and Y. Wang, Chin. Opt. Lett. **7,** 849 (2009).
6. L. W. Li, Y. N. Li, T. S. Yeo, J. R. Mosig, and O. J. F. Martin, Appl. Phys. Lett. **96,** 164101 (2010).
7. J. Valentine, S. Zhang, and T. Zenetgraf, Nature **455,** 376 (2008).
8. S. P. Burgos, R. de Waele, and A. Polman, Nature Materials **9,** 407 (2010).
9. P. Neutens, L. Lagae, and G. Borghs, Nano Lett. **10,** 1429 (2010).
10. M. D. He, J. Q. Liu, Z. Q. Gong, Y. F. Luo, X. Chen, and W. Lu, Opt. Commun. **283,** 1784 (2010).
11. X. Jin, X. Huang, J. Tao, X. Lin, and Q. Zhang, IEEE Trans. Nanotechnol. **9,** 134 (2010).
12. K. T. Kim, H. W. Kwon, J. W. Song, S. Lee, W. G. Jung, and S. W. Kang, Opt. Commun. **180,** 37 (2000).
13. I. V. Shadrivov, A. A. Sukhorukov, Y. S. Kivshar, A. A. Zharov, A. D. Boardman, and P. Egan, Phys. Rev. E **69,** 016617 (2004).
14. I. V. Shadrivov, A. A. Sukhorukov, and Y. S. Kivshar, Phys. Rev. E **67,** 057602 (2003).
15. B. Wu, T. M. Grzegorczyk, Y. Zhang, and J. A. Kong, J. Appl. Phys. **93,** 9386 (2003).
16. J. Zhang, Y. He, C. Li, and F. Zhang, Acta Opt. Sin. (in Chinese) **29,** 2673 (2009).
17. Y. He, J. Zhang, and C. F. Li, J. Opt. Soc. Am. B **25,** 2081 (2008).
18. Z. H. Wang, Z. Y. Xiao, and W. Y. Luo, J. Opt. A: Pure Appl. Opt. **11,** 015101 (2009).
19. Y. He, Z. Q. Cao, and Q. S. Shen, Opt. Commun. **245,** 125 (2005).
20. S. G. Mao, M. S. Wu, Y. Z. Chueh, and C. H. Chen, IEEE Trans. Microw. Theory Tech. **53,** 3460 (2005).
21. R. A. Shelby, D. R. Smith, and S. Schultz, Science **292,** 77 (2001).